Letters in Drug Design & Discovery 23 (2026) 100366

Contents lists available at ScienceDirect

Letters in Drug Design & Discovery

journal homepage: www.keaipublishing.com/en/journals/lddd/

Potent α-glucosidase and tyrosinase inhibition by thiophene-based Schiff bases: Experimental and computational evaluation

Emel Ekinci[a,*,1], Kübra Öztürk[b,2], Özlem Gündoğdu Aytaç[c], Sertan Aytaç[c,3], Harun Çiftçi[d,4]

[a] Çankiri Karatekin University, Central Research Laboratory Application and Research Center, Çankırı, Türkiye
[b] Department of Genetics and Bioengineering, Faculty of Engineering and Architecture, Kırşehir Ahi Evran University, Kırşehir, Türkiye
[c] Department of Food Technology, Kaman Technical and Vocational School, Kirşehir Ahi Evran University, Kırşehir, Kaman, Türkiye
[d] Department of Medical Biochemistry, Faculty of Medicine, Kırşehir Ahi Evran University, Kırşehir, Türkiye

ARTICLE INFO

Keywords:
Thiophene
Schiff base
Diabetes
Hyperpigmentation
Enzyme inhibition
Molecular docking
ADME

ABSTRACT

In this study, novel thiophene-based Schiff base derivatives were synthesized, and their structures were comprehensively analyzed. The inhibitory potentials of these compounds on α-glucosidase and tyrosinase enzymes were systematically evaluated. Among the thiophene-based Schiff bases, compound **8** exhibited moderate inhibitory activity against both α-glucosidase and tyrosinase, with IC_{50} values of 173.29 and 69.32 μM for each, compared to the positive controls acarbose and kojic acid, respectively. The DFT approach was used to analyze the reactivity and molecular electrostatic potential maps of the compounds, and molecular docking studies for the most active compounds **4**, **6**, and **8** were conducted on both the fungal tyrosinase and Saccharomyces cerevisiae protein models. Furthermore, ADME (Absorption, Distribution, Metabolism, and Excretion) analyses were performed to evaluate their pharmacokinetic profiles and predict their potential bioavailability with basic drug-like properties, and these observations demonstrate the potential importance of the compounds in the field of treating diabetes and skin diseases.

1. Introduction

Research into new enzyme inhibitors with therapeutic potential has become a fundamental area of medicinal chemistry, especially in the context of metabolic and dermatological disorders. Diabetes mellitus (DM) is a major endocrine disorder characterized by chronic hyperglycemia resulting from insufficient insulin secretion and impaired glucose metabolism[1–3]. Diabetes mellitus is classified into three main types: type 1 diabetes, type 2 diabetes, and gestational diabetes. Type 1 diabetes is characterized by an absolute deficiency of insulin resulting from autoimmune destruction of pancreatic β-cells, whereas type 2 diabetes initially develops through

* Corresponding author.
E-mail addresses: emelekinci@karatekin.edu.tr (E. Ekinci), kubra.ozturk@ahievran.edu.tr (K. Öztürk), ogundogdu@ahievran.edu.tr (Ö.G. Aytaç), saytac@ahievran.edu.tr (S. Aytaç), hciftci@ahievran.edu.tr (H. Çiftçi).
[1] https://orcid.org/0000-0003-2323-2747
[2] https://orcid.org/0000-0002-4488-0164
[3] https://orcid.org/0000-0002-3196-4545
[4] https://orcid.org/0000-0002-3210-5566

https://doi.org/10.1016/j.lddd.2026.100366
Received 27 November 2025; Received in revised form 26 December 2025; Accepted 30 December 2025
Available online 12 March 2026

metabolic alterations that lead to insulin resistance in target tissues[4]. In addition to metabolic, genetic, and environmental factors, inflammatory mediators have also been shown to play a significant role in the pathogenesis of both type 1 and type 2 diabetes[2,5]. Type 2 Diabetes Mellitus (T2DM) is a global disease that negatively impacts individuals' quality of life and poses a serious economic burden on healthcare systems[6,7]. In 2021, it was estimated that around 550 million people aged between 20 and 79 were living with diabetes, and this number is expected to reach 800 million by 2045. As the number of patients increases, diabetes-related healthcare costs are also anticipated to rise; diabetes-related health expenses, calculated at $966 billion in 2021, are projected to hit $1.054 trillion by 2045. This situation represents a significant economic burden not only on individual health but also on global healthcare systems[8,9]. Various strategies have been developed to manage postprandial hyperglycemia in T2DM. One of these strategies is the inhibition of enzymes that play a crucial role in carbohydrate metabolism. Specifically, the inhibition of the enzyme α-glucosidase, which facilitates the breakdown of di- and polysaccharides into glucose in the intestinal lumen, contributes to a more balanced regulation of blood sugar levels by delaying glucose absorption[10]. Therefore, the α-glucosidase enzyme is considered an important target in the treatment of T2DM and has become one of the priority research topics in the development of potential pharmacological agents[11].

In this context, enzyme inhibition emerges as an important strategy not only in the management of metabolic diseases but also in dermatoses. α-Glucosidase inhibition offers an effective approach in diabetes treatment, while similarly, tyrosinase inhibition plays a critical role in controlling hyperpigmentation[12]. Hyperpigmentation occurring in human skin is often an undesirable condition, and the primary reason for this phenomenon is the enzyme tyrosinase, which is the main regulator of the melanogenesis process.[13]. Excessive melanin production and pigment accumulation are commonly seen in various dermatological conditions such as periorbital hyperpigmentation, acanthosis nigricans, and cervical poikiloderma[14]. While the process of melanogenesis involves a quite complex biochemical mechanism, the enzyme tyrosinase plays a critical role in melanin biosynthesis by oxidizing dopamine to facilitate melanin formation. However, increased melanin production in the brain has been linked to Parkinson's disease and other neurodegenerative disorders.[15,16]. On the other hand, the number of compounds that can effectively inhibit tyrosinase is quite limited. Therefore, the demand for tyrosinase inhibitors is increasing every day in the medical and cosmetic fields[15].

It is believed that the multiple hydroxyl groups found in polyphenols enhance their inhibitory effects due to their ability to form stronger bonds with enzymes[17]. Under suitable conditions, inhibitor molecules can interact with enzymes and hinder their activities. Various studies have reported that both synthetic and natural polyphenols possess a range of biological activities, such as α-glucosidase and tyrosinase inhibition[13,18,19].

Heterocyclic compounds are defined as organic molecules that possess ring systems containing heteroatoms such as nitrogen, oxygen, or sulfur, in addition to carbon atoms. Such structures hold significant importance in modern drug design due to the high specificity they provide during interaction with biological targets[20].Compounds containing heteroatoms form the basic skeletons of numerous naturally occurring and biologically active molecules, and thanks to this property, they are widely used in medicinal chemistry for the development of new drug candidates[21]. Nitrogen-containing heterocyclic compounds, which exhibit a wide range of biological activity, are of particular interest to researchers[22]. The knowledge of the antibacterial, antiallergic, and chemotherapeutic effects of sulfur-containing compounds has increased research into the synthesis of these compounds[23]. In this context, various thiophene derivatives have been designed as drugs or drug candidates, and compounds containing a thiophene ring as a pharmacophore in their structure have been reported to exhibit numerous biological activities such as anti-asthmatic, diuretic, anticancer, antibacterial, anti-HIV, and anticonvulsant properties[24,25]. In addition, nitrogen-containing heterocyclic compounds are widely found both in nature and in pharmaceutical products, exhibiting significant biological activities such as anticancer, antimicrobial, analgesic, and anti-inflammatory properties[26]. In recent years, various Schiff bases containing N, O, S, and P atoms in their structures have been synthesized and evaluated in biological applications[27–29]. Schiff bases are known to have a broad biological activity profile in the pharmaceutical industry due to the imine group in their structure[30]. The synthesis of thiophene-based Schiff bases, in particular, has attracted increasing attention recently due to their biological importance[26,28].

Schiff bases, characterized by the azomethine (-CH = N) functional group, are widely recognized for their diverse biological and industrial applications, including antibacterial, antihypertensive, antipyretic, anticancer, anti-inflammatory, and anti-HIV activities[31,32]. Particularly, thiophene-based Schiff bases, which incorporate sulfur into their heterocyclic framework, exhibit significant pharmacological potential due to their electron-rich nature, structural flexibility, and bioisosteric relationship with benzene, making them highly relevant in drug discovery and material science[33]. The presence of thiophene enhances lipophilicity, bioavailability, and metabolic stability, which is why it forms the core structure of various marketed drugs such as olanzapine (antipsychotic), dorzolamide (anti-glaucoma), duloxetine (antidepressant), tiotropium (bronchodilator), and clopidogrel (antithrombotic agent)[34–36] (Scheme 1). Given these developments, further research into thiophene derivatives may lead to the development of more effective and selective enzyme inhibitors for therapeutic use.

Furthermore, Schiff bases containing phosphonate groups have gained considerable interest due to their structural similarity to α-amino acids, where the carboxyl group is replaced by a phosphonic acid moiety, enabling them to act as enzyme inhibitors, anticancer agents, antioxidants, antiviral compounds, and plant growth regulators[37–39]. Given their extensive pharmacological and industrial significance, the synthesis and characterization of novel thiophene and phosphonate-based Schiff bases hold promising prospects for future advancements in medicinal chemistry, material science, and pharmaceutical applications.

In this study, four compounds previously reported in the literature and two new derivatives containing phosphate groups were synthesized for the first time. Compounds **4–7** were synthesized in the literature by different methods[40–44]. The synthesis of compounds **4–5** was synthesized for the first time with an environmentally friendly method in a shorter time, without solvents, and with high yields. According to literature data, compounds containing sulfur in their structure are known to possess various biological activities[45]. In this context, considering the potential biological activities of Schiff bases, new thiophene-based Schiff bases were first

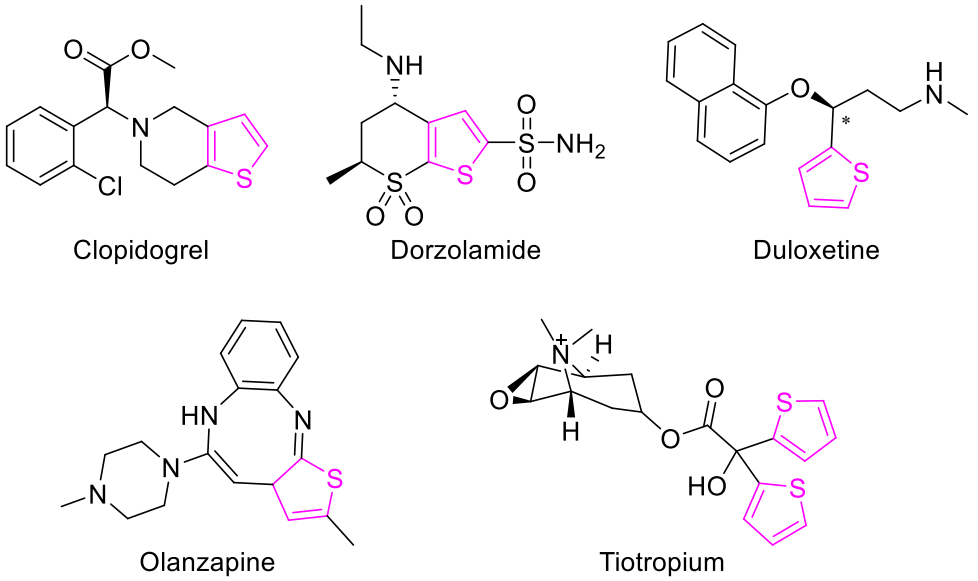

Scheme 1. Some commercially available drugs contain a thiophene ring.

synthesized, followed by the preparation of their reduction products[30]. Based on the hypothesis that incorporating multiple biologically active cores within a molecule could contribute to the development of new compound classes with significant biological activities[46], the α-aminophosphonate derivatives of the synthesized thiophene-based Schiff bases were also synthesized[27]. Then, the effect of the synthesized compounds (**4–9**) on biological activity was investigated. The inhibitory effects of a total of six synthesized compounds on α-glucosidase and tyrosinase enzymes were evaluated for the first time; the results revealed that especially the newly synthesized phosphate derivatives could show significant inhibitory effects on these enzymes. The selected molecular scaffolds include heterocycles containing thiazole, benzothiazole, and phosphorus, which have been comprehensively reported for their biological activities. These heterocyclic structures were chosen based on their well-documented enzyme inhibition properties, strong binding affinities to key enzymatic residues, and favorable pharmacokinetic characteristics that enhance drug-likeness. To further validate the effectiveness of the synthesized compounds, in vitro enzyme inhibition assays were conducted, and molecular docking simulations were performed to elucidate the binding mechanisms. Additionally, ADME (Absorption, Distribution, Metabolism, and Excretion) studies were carried out to evaluate their pharmacokinetic profiles and drug likeness. This comprehensive approach integrates experimental findings with computational modeling, providing valuable insights into the potential therapeutic applications of the synthesized compounds.

2. Materials and methods

2.1. Chemicals and apparatus

The chemicals used in this study were obtained from Sigma-Aldrich and Merck (USA). Enzymes, substrates, inhibitors, and other reagents used in enzyme activity studies were obtained from Sigma-Aldrich. Melting points of the solid products were measured with Gallenkamp melting point instruments. ^{1}H NMR and ^{13}C NMR spectra were performed on 400 (100)-MHz Varian and Bruker spectrometers, and elemental analyses were performed on a Leco CHNS-932 instrument.

2.2. General synthesis of Schiff bases

Schiff bases **7–11** were synthesized using the protocols indicated in the literature[47,48]. Thiophene-2-carboxyaldehyde (**1**) (1 mmol) was added to 4-methoxyaniline (**2**) and p-toluidine (**3**) (1 mmol), and then the reaction mixture was exposed to microwave radiation at 900 W for 5 min (Scheme 2). The progress of the reactions was followed by TLC. Both the ^{1}H and ^{13}C NMR spectra pointed to the formation of a single product.

2.2.1. Synthesis of 4-methoxy /methyl -N-(thiophen-2-ylmethyl)aniline (6 − 7)

4-methoxy/methyl-N-N-*N*-(thiophen-2-ylmethyl)aniline (**6–7**) was synthesized by making some modifications to the procedures given in the literature[28,49]. After *N*-(4-methoxy/methylphenyl)-1-(thiophen-2-yl) methanimine **(4 − 5)** (1 equiv.) was dissolved in THF/H_2O (1:1, 20 mL), $NaBH_4$ (8 equiv.) was added slowly at 0 °C (Scheme 3). The reaction mixture was stirred at room temperature for 6 h. The progress of the reaction was monitored by TLC, and after the reaction was complete, the solvent was removed using a rotary evaporator, and the compound was purified by crystallization.

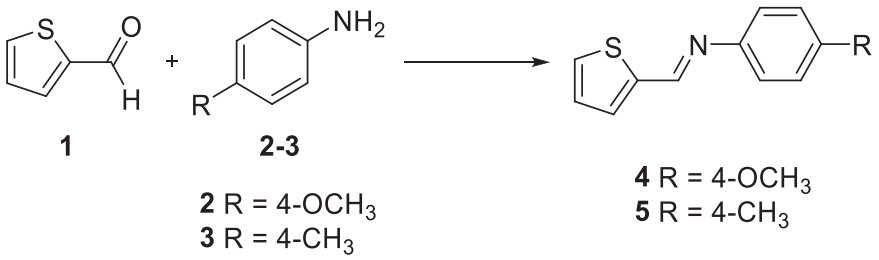

Scheme 2. General procedure for the synthesis of Schiff bases **4–5.**

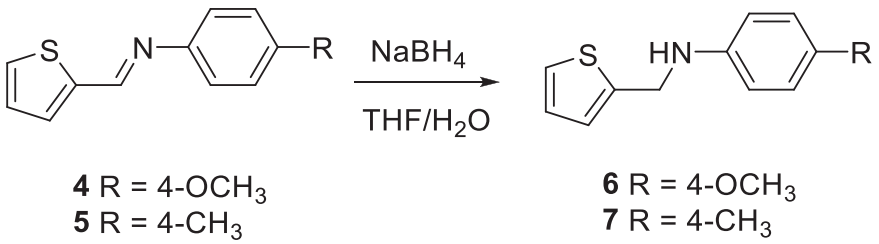

Scheme 3. General procedure for the synthesis of 4-methoxy/methyl-N-(thiophen-2-ylmethyl)aniline **(6 − 7).**

2.2.2. Synthesis of α-aminophosphonates (8 − 9)

The Schiff base compounds **4–5** (1 equiv.) were dissolved in ethanol, and diphenyl phosphonate (1 equiv.) was added gradually at room temperature. The reaction mixture was stirred continuously until a white precipitate formed. After the precipitation process, the filtrate was carefully separated, and the solid residue was allowed to air dry at ambient temperature (Scheme 4). This transformation proceeds via an aza-Pudovik (hydrophosphonylation) reaction, involving the nucleophilic addition of diphenyl phosphonate to the electrophilic C═N bond of the Schiff base, a well-established approach for the synthesis of α-aminophosphonates under mild conditions[27,50].

2.3. Enzyme activity studies

2.3.1. Determination of α-glucosidase activity

The α-glucosidase enzyme inhibition effects for new Schiff base derivatives (**4–9**) were analysed with a microtiter plate reader in accordance with the method previously described in the literatüre[51]. In this reaction, 4-Nitrophenyl-α-D-glucopyranoside was preferred as substrate. The enzyme solution was freshly prepared in cold deionised water containing 0.15–0.3 units/mL alpha-glucosidase. In the analysis procedure, 50 µL of phosphate buffer solution (1.0 M, pH 6.8), 50 µL of the new compound at different concentrations, and 10 µL of enzyme solution were added to the microplate well. After the mixture was incubated at 25 °C for 15 min, the reaction was initiated by adding 20 µL of 5 mM substrate solution. To determine the enzymatic activity, the absorbance change in the wells was recorded at A_{408} nm wavelength for 10 min.

2.3.2. Determination of tyrosinase enzyme activity

The tyrosinase enzyme inhibition potentials of the compounds were measured at 492 nm wavelength using a microtiter plate reader.[52]. Fungal tyrosinase enzyme was used in the experiments. For the enzyme activity assay, 125 µL of reaction medium was

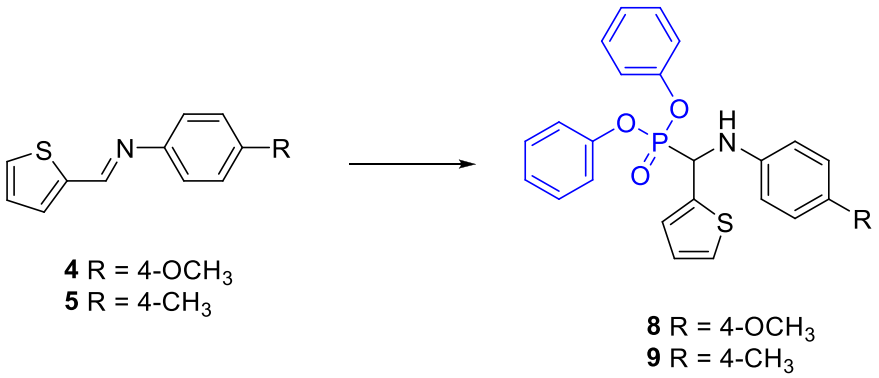

Scheme 4. General procedure for the synthesis of α-aminophosphonates compounds **8–9**.

prepared in 50 mM phosphate buffer (pH 6.8). The solution contained 0.5 mM L-DOPA and 50 μL of compound solution at different concentrations. The reaction was carried out by incubation at 37 °C for 7 min.

In both tests, the compounds were dissolved in DMSO at a concentration of 1 mg/mL and then diluted with distilled water to the appropriate concentration. In the control groups, an amount of %10 (v/v) DMSO equal to the ratio of the compound solutions in the reaction mixture was also included. In the experiments, acarbose was used as a positive control for α-glucosidase, and kojic acid was used as a positive control for tyrosinase enzyme.

The enzyme inhibition potentials of the compounds were calculated using slope formulas from the % activity and concentration plots. Enzyme activity was determined as percentage (%) activity relative to the inhibitor-free control group, based on Formula 1.

$$\%Activity = \frac{\text{Sample absorbance change}}{\text{Control absorbance change}} \text{x100} \quad (1)$$

The inhibitory effects of the compounds on α-glucosidase and tyrosinase activity were expressed as concentrations inhibiting 50% of the enzyme activity (IC_{50}).

2.4. Theoretical studies

2.4.1. Global reactivity descriptors

The molecular geometry optimization and harmonic vibration frequency calculations were performed using the density functional theory (DFT) approach with the B3LYP[53,54] functional and the cc-pVDZ[55] basis set. Global reactivity parameters are substantial quantum chemical descriptors that help in understanding the chemical reactivity and kinetic stability of molecules. These parameters offer estimation into the electronic characteristics of molecules and their interactions with biological receptors. All quantum chemical calculations were conducted using the Gaussian 16 software.

2.4.2. Molecular docking analysis

A molecular docking study was performed using Molegro Virtual Docker[56] to investigate the binding interactions of the most potent compounds within the active sites of α-glucosidase and tyrosinase. During the conformational search process, the MolDock SE algorithm was applied, and 10 independent simulations were conducted for each ligand. The default settings of the program were used for other docking parameters. The crystal structures of tyrosinase (PDB Kimliği:2Y9X çözünürlük: 2.78 Å) and α-glucosidase (PDB Kimliği: 3A4A, çözünürlük: 1,60 Å) enzymes were obtained from the Protein Data Bank (PDB). During the molecular docking process, the grid center was created at the coordinates (X: −10.00, Y: −28.92, Z: −43.83) for tyrosinase and (X: 15.04, Y: −8.48, Z: 18.10) for α-glucosidase. The grid spacing was fixed at 0.300 Å for both enzymes. Finally, the enzyme-ligand complexes with the best binding energy were visualized in two-dimensional and three dimensions using Discovery Studio Visualizer software.

2.4.3. ADMET prediction

Computer-aided ADMET calculations assist in evaluating a compound's potential for drug development and contribute to more cost-effective drug discovery and development processes. One of the web-based tools designed for analyzing ADMET properties, ADMETlab 2.0[57], was used to determine the ADMET profiles of all compounds. Additionally, certain ADMET parameters were calculated using the online platform http://www.swissadme.ch[58].

3. Results and discussion

3.1. Chemical results

The structures of new synthesized compounds **4–9** were characterized by ^{1}H NMR, ^{13}C NMR, and elemental analysis data. Two new thiophene-based Schiff bases were synthesized by using Thiophene-2-carboxyaldehyde (**1**), 4-methoxyaniline (**2**), and p-toluidine (**3**), and reacting them with microwave irradiation without using a solvent. This method is a cheap, fast, and environmentally friendly method, and both compounds (**4–5**) were obtained successfully with a high yield (96%). The characteristic proton in the H–C=N bond in compound number **4** formed a peak at 8.60 ppm in ^{1}H NMR spectra, and the characteristic proton in the H–C=NH–C=N bond in compound number **5** formed a peak at 8.61 ppm. In addition, the 151.13 and 152.31 ppm peaks in the ^{13}C NMR spectra indicate the carbon atoms in the H–C=N bond in compounds number **4** and **5**, respectively.

The reduction reactions of the synthesized Schiff bases (**4–5**) were also investigated, and 4-methoxy/methyl-N-(thiophen-2-yl-methyl)aniline (**6–7**) compounds were obtained with 94% and 95% yield, respectively. The disappearance of specific imine peaks and the emergence of -CH_2 peaks at 4.51 (s, 2 H, CH_2) and 4.50 (s, 2 H, CH_2) ppm as a result of the reduction reaction of imine compounds **4** and **5** indicate that the reduction reactions were successful. When the ^{13}C NMR spectra were also examined, it was seen that the newly formed -CH_2 peaks gave signals at 44.50 and 49.54 ppm.

In the compounds obtained by adding diphenyl phosphonate to Schiff bases, -CH-$PO(OPh)_2$ peaks appeared at 5.36 and 5.43 ppm. When the ^{13}C NMR spectra were also examined, the newly formed -CH_2 peaks gave signals at 53.95 and 52.28 ppm.

3.2. Physical properties and spectral data of synthesized compounds (4 – 9)

***N*-(4-methoxyphenyl)-1-(thiophen-2-yl)methanimine (4):** Yield: 96%, brown solid, m.p. 49–51 °C. **^{1}H NMR** (400 MHz, $CDCl_3$) δ 8.60 (s, 1 H), 7.52 – 7.45 (m, 2 H), 7.28 – 7.23 (m, 2 H), 7.16 – 7.12 (m, 1 H), 6.97 – 6.92 (m, 2 H), 3.84 (s, 3 H). **^{13}C NMR** (100 MHz, $CDCl_3$) δ 158.32, 151.13, 144.36, 143.20, 131.59, 129.76, 127.72, 122.29, 114.39, 55.49. **Chemical Formula**: $C_{12}H_{11}NOS$. **Elemental Analysis:** C, 66.33; H, 5.10; N, 6.45. **Found:** C, 66.30; H, 5.14; N, 6.49.

1-(thiophen-2-yl)-*N*-(p-tolyl)methanimine (5): Yield: 96%, yellow solid, m.p. 65–66 °C. **^{1}H NMR** (400 MHz, $CDCl_3$) δ 8.61 (s, 1 H), 7.58 – 7.45 (m, 2 H), 7.25 – 7.13 (m, 5 H), 2.40 (s, 3 H). **^{13}C NMR** (100 MHz, $CDCl_3$) δ 152.31, 148.85, 143.03, 135.94, 131.96, 130.07, 129.80, 127.75, 120.96, 21.08. **Chemical Formula**: $C_{12}H_{11}NS$. **Elemental Analysis:** C, 71.61; H, 5.51; N, 6.96 **Found:** C, 71.64; H, 5.47; N, 6.98.

4-methoxy-*N*-(thiophen-2-ylmethyl)aniline (6): Yield: 94%, white solid, m.p. 73–75 °C. (m.p. 70–72)[41]. **^{1}H NMR** (400 MHz, $CDCl_3$) δ 7.26 (d, J = 4.7 Hz, 1 H), 7.11 – 6.98 (m, 2 H), 6.86 (d, J = 8.4 Hz, 2 H), 6.72 (t, J = 14.9 Hz, 2 H), 4.51 (s, 2 H), 3.80 (s, 3 H). **^{13}C NMR** (100 MHz, $CDCl_3$) δ 152.57, 143.44, 141.91, 126.89, 124.96, 124.57, 114.91, 114.65, 55.77, 44.50. **Chemical Formula**: $C_{12}H_{13}NOS$. **Elemental Analysis:** C, 65.72; H, 5.98; N, 6.39. **Found:** C, 65.76; H, 5.94; N, 6.41.

4-methyl-*N*-(thiophen-2-ylmethyl)aniline (7): Yield: 95%, orange solid, m.p. 82–84 °C (m.p. 85–86)[41]. **^{1}H NMR** (400 MHz, $CDCl_3$) δ 11.52 (s, 1 H, NH), 7.23 – 7.11 (m, 4 H), 7.05 (d, J = 8.2 Hz, 2 H), 6.87 – 6.79 (m, 1 H), 4.50 (s, 2 H), 2.24 (s, 3 H). **^{13}C NMR** (100 MHz, $CDCl_3$) δ 139.44, 131.77, 131.40, 130.38, 130.25, 128.14, 127.44, 123.65, 49.54, 21.12. **Chemical Formula**: $C_{12}H_{13}NS$. **Elemental Analysis:** C, 70.90; H, 6.45; N, 6.89; S, 15.77. **Found:** C, 70.95; H, 6.41; N, 6.92.

Diphenyl (((4-methoxyphenyl)amino)(thiophen-2-yl)methyl)phosphonate (8): Yield: 89%, white solid, m.p. 129.5 °C. **^{1}H NMR** (400 MHz, $CDCl_3$) δ 7.35 – 7.25 (m, 6 H), 7.23 – 7.11 (m, 4 H), 7.02 (dd, J = 8.6, 4.0 Hz, 3 H), 6.84 – 6.67 (m, 4 H), 5.36 (d, J = 23.9 Hz, 1 H), 3.81 – 3.70 (m, 3 H). **^{3}C NMR** (100 MHz, $CDCl_3$) δ 153.43, 150.42d, 150.30d, 139.70, 139.56, 138.65, 129.74 d, 127.32d,127.00, 126.92, 125.86d, 125.8d, 120.70d, 120.42 d, 115.90, 114.84, 55.64, 53.95d. **Chemical Formula**: $C_{24}H_{22}NO_4PS$ **Elemental Analysis:** C, 63.85; H, 4.91; N, 3.10 **Found:** C, 63.81; H, 4.96; N, 3.15.

Diphenyl (thiophen-2-yl(p-tolylamino)methyl)phosphonate (9): Yield: 91%, white solid, m.p. 147.7 °C. **^{1}H NMR** (400 MHz, $CDCl_3$) δ 7.35 – 7.26 (m, 6 H), 7.23 – 7.11 (m, 4 H), 7.02 (t, J = 7.1 Hz, 5 H), 6.68 (t, J = 5.4 Hz, 2 H), 5.43 (d, J = 24.2 Hz, 1 H), 2.27 (s, 3 H). **^{13}C NMR** (100 MHz, $CDCl_3$) δ 150.38d, 150.28d, 143.40, 143.26, 138.58, 129.88, 129.77, 128.74, 127.33d, 127.01, 126.94, 125.86d, 125.41d, 120.72d, 120.44d, 114.40, 52.28d, 20.50. **Chemical Formula**: $C_{24}H_{22}NO_3PS$ **Elemental Analysis:** C, 66.19; H, 5.09; N, 3.22 **Found:** C, 66.13; H, 5.13; N, 3.26.

3.3. Enzyme activity studies's results

The *in vitro* enzyme inhibitory activities of the synthesized compounds **4–9** against α-glucosidase and tyrosinase were evaluated. The data obtained revealed that the compounds exhibited different inhibitory effects on *α*-glucosidase and tyrosinase enzymes (Table 1). Acarbose was used as positive control for *α*-glucosidase, and kojic acid was used as positive control for tyrosinase enzyme**.**

When the inhibitory effects of the synthesized compounds **4–9** on the tyrosinase enzyme were evaluated, it was determined that compound **9** did not show any inhibitory effect. However, IC_{50} values of compounds **5** and **7** were calculated as 173.29 μM and 231.05 μM, respectively. For compounds **4–8**, IC_{50} values ranged between 128.30 and 69.32 μM. Among the synthesized compounds, compound **8** containing methoxy and α-aminophosphonate groups exhibited the lowest IC_{50} value against tyrosinase (69.32 μM) within the series; however, its inhibitory activity remained weaker than that of the standard inhibitor kojic acid (Table 1). When compounds **8** and **9** containing the *α*-aminophosphonate group were compared, the addition of a methoxy group instead of a methyl group led to an increase in inhibition activity. The observation that the methoxy group increases the inhibition activity compared to the methyl group is in agreement with the literature describing the structural interactions of *α*-aminophosphonate compounds in enzyme inhibition. *α*-Aminophosphonates have strong binding ability thanks to their phosphonate groups in their interactions with enzymes, and the electron distribution of these groups plays a critical role in determining their inhibitory effects[59]. The electron-donating property of the methoxy group may enhance the polarity of the compound, leading to stronger interactions with the enzyme's active site[60]. Furthermore, studies on the binding capacities of aminophosphonate derivatives to specific enzymes such as PARP1 have shown that even minor structural changes can significantly alter the binding affinity and thus the inhibition activity[61]. Similarly, Rao et al. reported that the biological activity of derivatives containing electron-donating groups increased[62]. Previous studies have shown that hydroxyl and methoxy groups in polyphenols bind to the active site of tyrosinase and form chelates with

Table 1
Inhibitory effects of all compounds on α-glucosidase and tyrosinase enzymes.

Compound	Tyrosinase IC_{50} (μM)	α-Glucosidase IC_{50} (μM)
4	128.30	223.59
5	173.29	364.81
6	110.02	231.05
7	231.05	693.15
8	69.32	173.29
9	-	239.02
Kojic acid	**7.46**	-
Acarbose	-	**79.63**

copper ions, thus suppressing the activity of the enzyme[63]. Therefore, the stronger inhibition of enzyme activity with the addition of the methoxy group can be explained by the changes in the electronic properties of the compound and the mechanisms of interaction with the enzyme. Table 1 further demonstrates that the newly synthesized compounds exhibit weaker inhibitory activity against tyrosinase compared to kojic acid.

IC_{50} values of **4**, **5,** and **6** molecules, which are Schiff bases, were calculated as 223.59, 364.81, and 231.05 μM, respectively. On the other hand, IC_{50} values of **8** and **9** molecules, which are α-aminophosphonates, were calculated as 173.29 and 239.02 μM, respectively. According to the calculated IC_{50} values, molecule **8** containing methoxy and α-aminophosphonate groups showed the lowest IC_{50} value among the synthesized compounds against α-glucosidase; nevertheless, its activity was weaker than that of the reference inhibitor acarbose. Modification of thiophene-derived Schiff bases with aminophosphonate groups has been shown to increase α-glucosidase inhibition. This is attributed to the electron-donating nature of the aminophosphonate group, which increases the binding affinity by establishing stronger interactions with the enzyme active site.[64]. In the literature, there are various studies showing that α-aminophosphonates increase the inhibitory effect against α-glucosidase enzyme. For example, Kandula et al. synthesised α-aminophosphonate derivatives containing piperazine and 1,2,3-triazole and investigated the inhibitory effects of these compounds against α-glucosidase. In their study, it was determined that the inhibition effect of all synthesised molecules against α-glycosidase was weaker compared to α-aminophosphonate derivatives. They also found that α-aminophosphonate derivatives showed a stronger inhibitory effect than acarbose (IC_{50}: 79.1 ± 0.05 μM), which is used as a reference inhibitory substance in the literature[65]. Similarly, Kumar et al. reported that aminophosphonate groups form stronger bonds with enzymes through hydrogen bonding and electrostatic interactions[66]. These results support that modification of thiophene-derived Schiff bases with aminophosphonates enhances α-glucosidase inhibition and such compounds may be considered as preliminary lead structures for further optimization toward anti-diabetic agents.

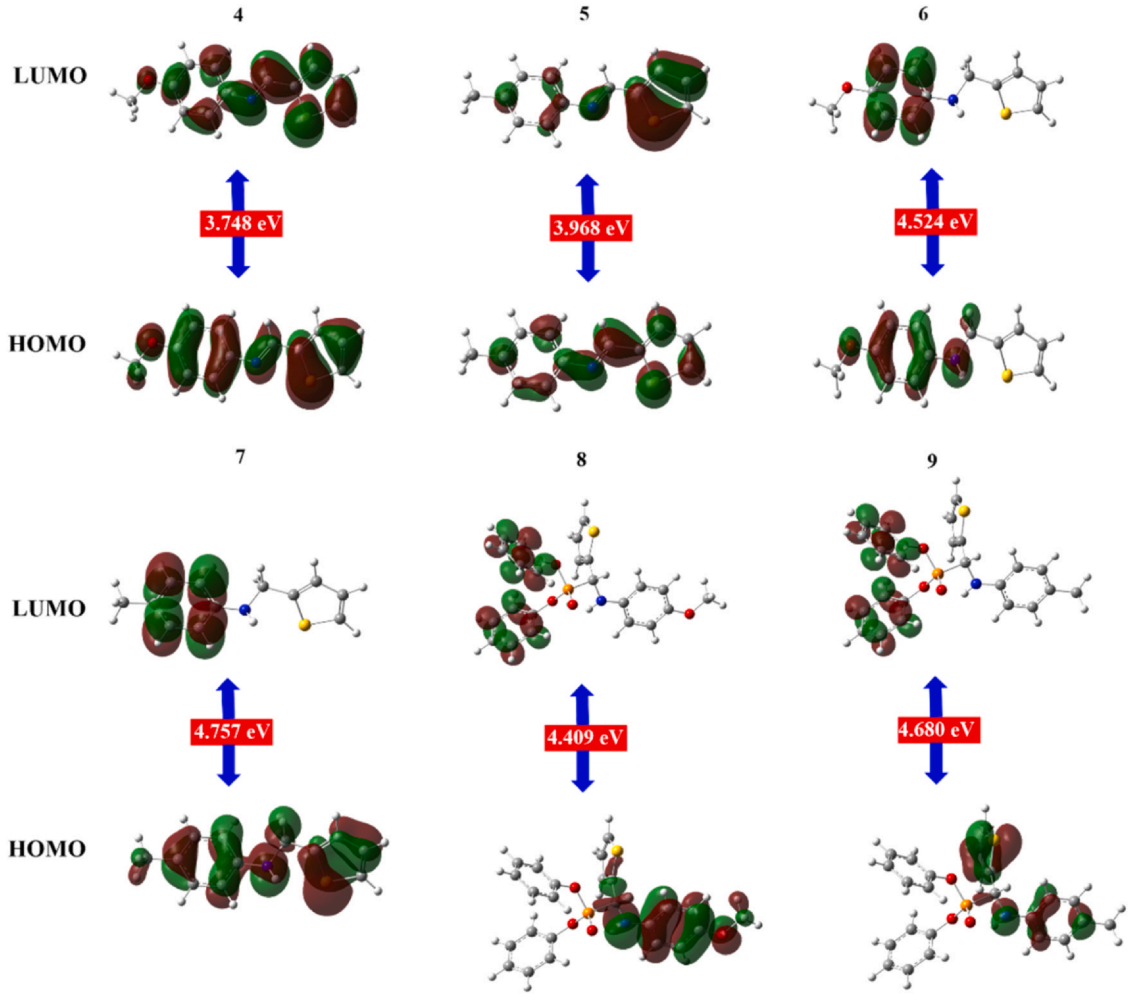

Fig. 1. The frontier molecular orbitals of compounds obtained at the B3LYP/cc-pVDZ level.

Table 2
Global reactivity parameters in (eV) for **4-9** compounds.

	HOMO	LUMO	Gap	IP	EA	μ	η	σ	χ	ω
4	-5.480	-1.732	3.748	5.480	1.732	-3.606	1.874	0.534	3.606	3.469
5	-5.782	-1.814	3.968	5.782	1.814	-3.798	1.984	0.504	3.798	3.636
6	-5.061	-0.537	4.524	5.061	0.537	-2.799	2.262	0.442	2.799	1.731
7	-5.330	-0.573	4.757	5.330	0.573	-2.951	2.379	0.420	2.951	1.831
8	-5.205	-0.797	4.409	5.205	0.797	-3.001	2.204	0.454	3.001	2.043
9	-5.483	-0.803	4.680	5.483	0.803	-3.143	2.340	0.427	3.143	2.111

*Softness, σ, is given in $(eV)^{-1}$.

3.4. Molecular modeling studies's results

3.4.1. Global reactivity descriptors

Global reactivity parameters (GRPs) are determined based on the energies of the highest occupied molecular orbital (HOMO) and the lowest unoccupied molecular orbital (LUMO). These orbitals play a crucial role in quantum chemistry, influencing various molecular properties, including ionization potential (I), electron affinity (A), electronegativity (χ), chemical potential (μ), chemical hardness (η), chemical softness (σ), and electrophilicity (ω). A compound's chemical reactivity can be analyzed by studying the energy values of the HOMO and LUMO. The difference in energy between these orbitals serves as a key factor in understanding their reactivity[67]. Fig. 1 displays the 3D representations of the HOMO and LUMO for the compounds. Table 2 provides the global reactivity descriptors for compounds **4–9**, offering valuable insights into their electronic characteristics. A higher E_{HOMO} value signifies a greater electron-donating ability, whereas a lower E_{LUMO} value indicates a stronger tendency to accept electrons. Among the examined compounds, compound **5** has the highest E_{HOMO} at −5.782 eV, reflecting its strong electron-donating nature. Conversely, compound **6** exhibits the lowest E_{LUMO} at −0.537 eV, making it a more effective electron acceptor. Additionally, compound **5** possesses the highest electronegativity (χ), while compound **6** has the lowest χ value. The calculated electronegativity ranking follows the order: **5** > **4** > **9** > **8** > **7** > **6**. Furthermore, compound **5** demonstrates the highest electrophilicity index (ω), reinforcing its superior electrophilic behavior and its efficiency as an electron acceptor, whereas compound **6** primarily acts as an electron donor. Table 2 also reveals that the global hardness (η) values of the studied compounds are significantly greater than their global softness (σ) values. These results indicate that compounds **4–9** exhibit increased softness, reduced chemical stability, and enhanced reactivity compared to the other compounds analyzed.

3.4.2. Molecular electrostatic potential (MEP) maps

In a MEP map, red areas signify electron-rich regions with the highest negative potential, making them ideal for electrophilic attack. Conversely, blue regions indicate electron-deficient areas with positive potential, which are more susceptible to nucleophilic attack. Additionally, green areas correspond to regions with neutral potential. The potential follows a decreasing trend in the order: red < orange < yellow < green < blue[68]. The molecular electrostatic potential of the compounds was calculated using the B3LYP/cc-pVDZ approach, based on the optimized structure file (.chk). Fig. 2 presents the MEP map of the compounds **4–9**. An analysis of the

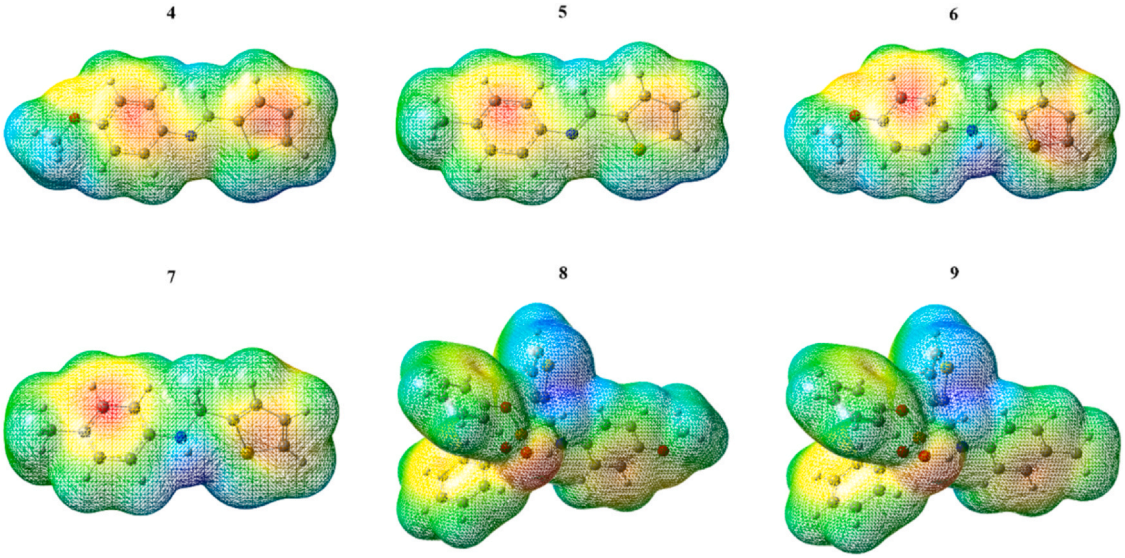

Fig. 2. Molecular electrostatic potential (MEP) map of compounds obtained at the B3LYP/cc-pVDZ level.

Table 3
Details regarding the binding interactions of compounds **4** and **8** within the α-glucosidase active site.

Types	Category	4	8
Hydrogen bond	Conventional Hydrogen Bond	Ser241, Asp242	Arg315, Ser241, Tyr158
Electrostatic	Pi–anion	-	Asp242
Hydrophobic	Pi–pi stacked	Tyr158	Tyr158
	Pi–alkyl	Arg315, Tyr158, Lys156	Arg315, Tyr158, Lys156
	Alkyl	Leu177	Leu177
	Sulfur	Phe314	-
Docking Score		-94.2087	-184.62

Table 4
Details regarding the binding interactions of compounds **6** and **8** within the tyrosinase active site.

Types	Category	6	8
Hydrogen bond	Conventional Hydrogen Bond	Met280	Asn260
Electrostatic	Pi–anion	-	Glu256
Hydrophobic	Pi–pi stacked	His263	His263
	Pi–alkyl	His244, Val283, Ala286	His85, Val283, Ala286
	Alkyl	Val248	Val283
	Sulfur	His61, His263	His263
Docking Score		-102.29	-115.453

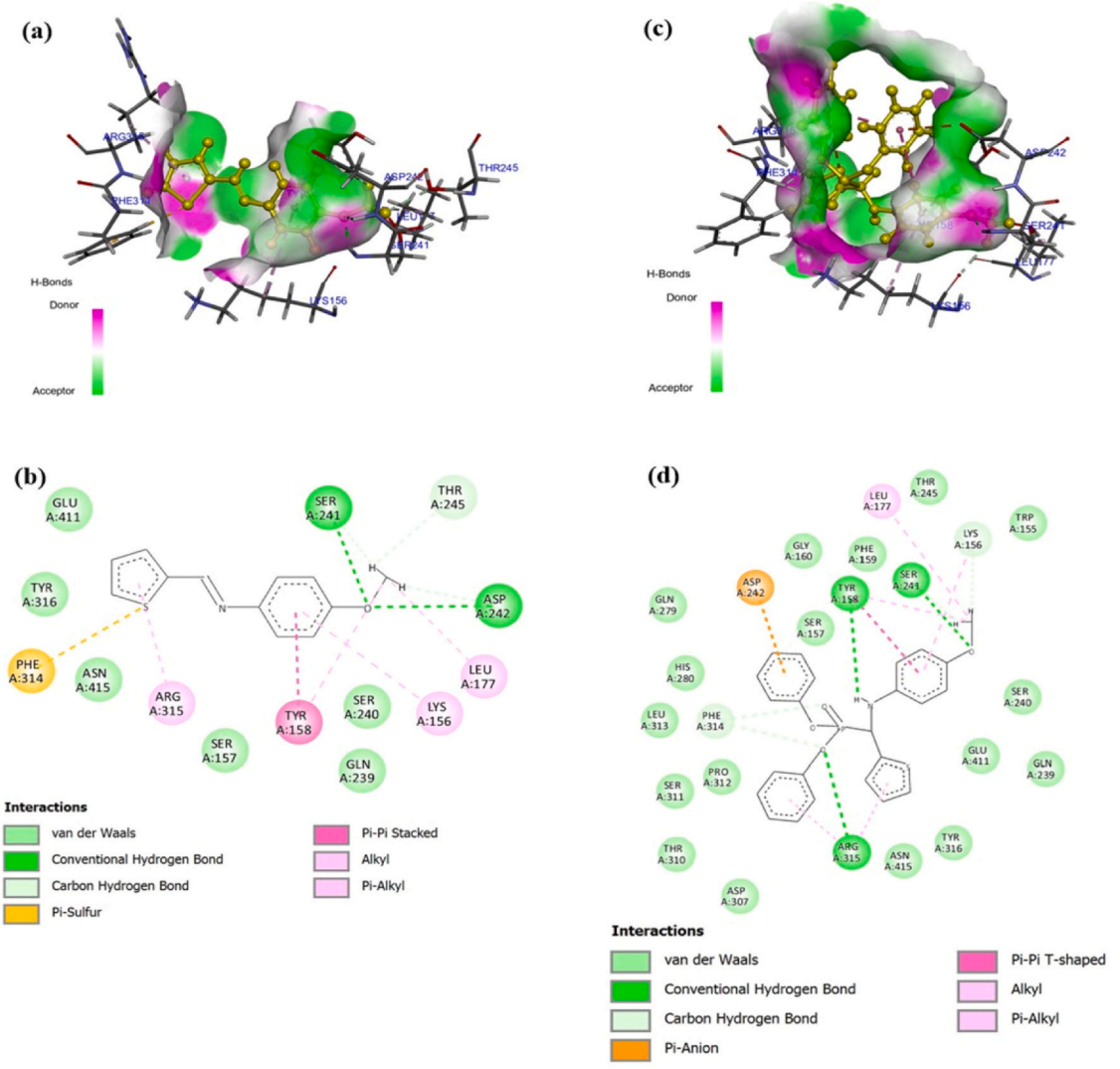

Fig. 3. The molecular docking results of the compound **4** & α-glycosidase, **a)** the surfaces around ligand (3D) and **b)** 2D forms, the molecular docking results of the compound **8** & α-glycosidase, **c)** the surfaces around ligand (3D) and **d)** 2D forms.

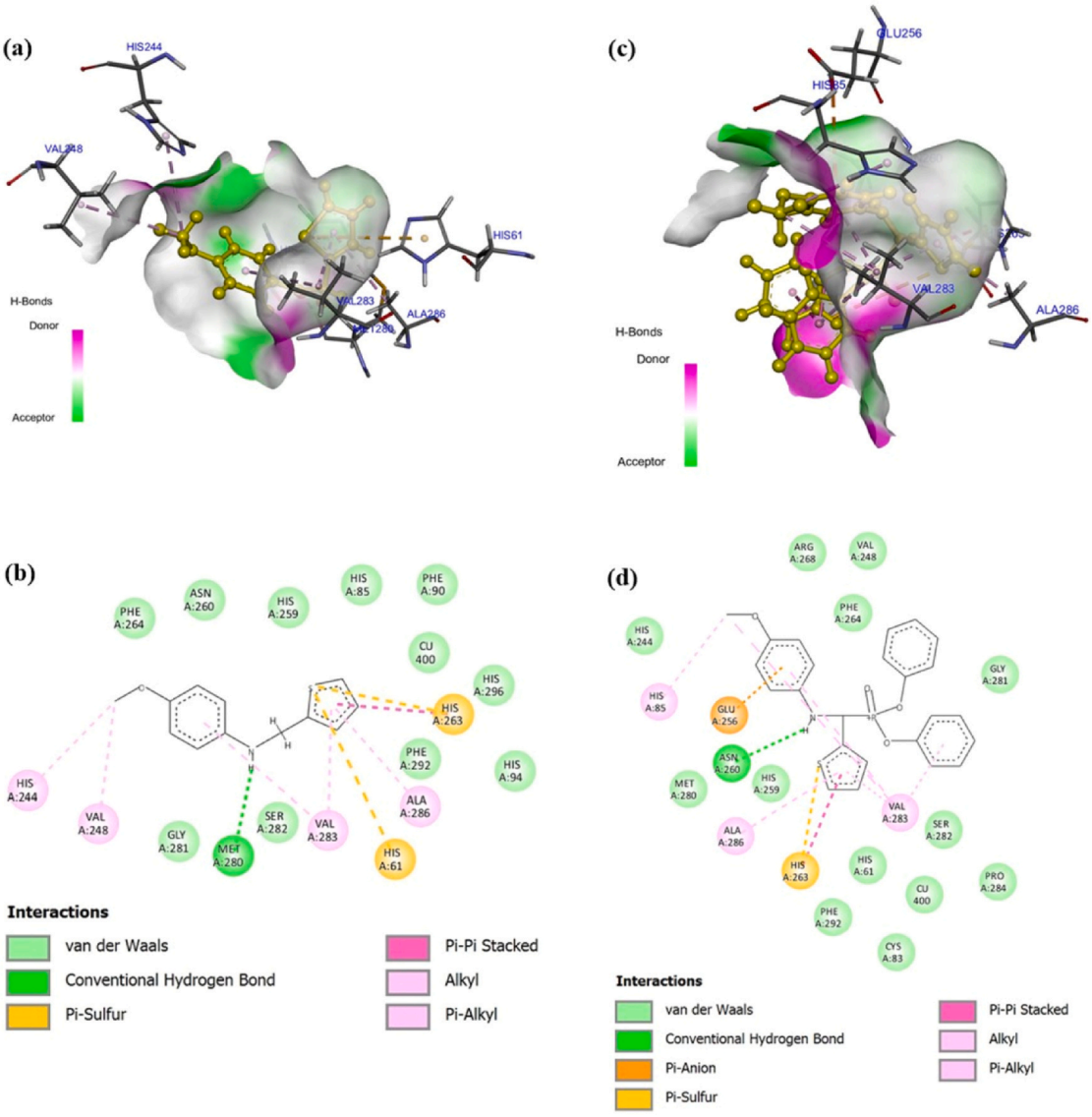

Fig. 4. The molecular docking results of the compound **6 & Tyrosinase a)** the surfaces around ligand (3D) and **b)** 2D forms, the molecular docking results of the compound **8 & Tyrosinase c)** the surfaces around ligand (3D) and **d)** 2D forms.

MEP maps for compounds **4–9** reveals that the benzene and thiophene rings contain the highest electron density. In contrast, the regions with the lowest electron density are found on the hydrogen atoms on the imine groups.

3.5. Molecular docking studies

To better understand the inhibitory mechanisms of compounds with low IC_{50} values, molecular docking studies were carried out for compounds **6** and **8** against the active site of tyrosinase, and for compounds **4** and **8** against the active site of glycosidase. The docking results, including binding affinities and interaction profiles, are comprehensively summarized in Tables 3 and 4. Binding models showing molecular interactions between tyrosinase and glycosidase enzymes and selected compounds are presented in Fig. 3 and Fig. 4.

Compound **4** exhibited a docking score of –94.2087. It established conventional hydrogen bonds with Ser241 and Asp242 and engaged in hydrophobic interactions with Tyr158, Arg315, Lys156, Leu177, and Phe314. Compound **8** demonstrated a docking score of –184.62. It formed conventional hydrogen bonds with Arg315, Ser241, and Tyr158, while hydrophobic interactions with Tyr158, Arg315, Lys156, and Leu177. Additionally, compound **8** displayed an electrostatic interaction with Asp242. The docking results show partial qualitative agreement with the observed IC_{50} trends, rather than a direct quantitative correlation. Residues such as Tyr158 and His280, together with loops 310–315, are located at the entrance to the active site of the glycosidase enzyme[69]. These residues

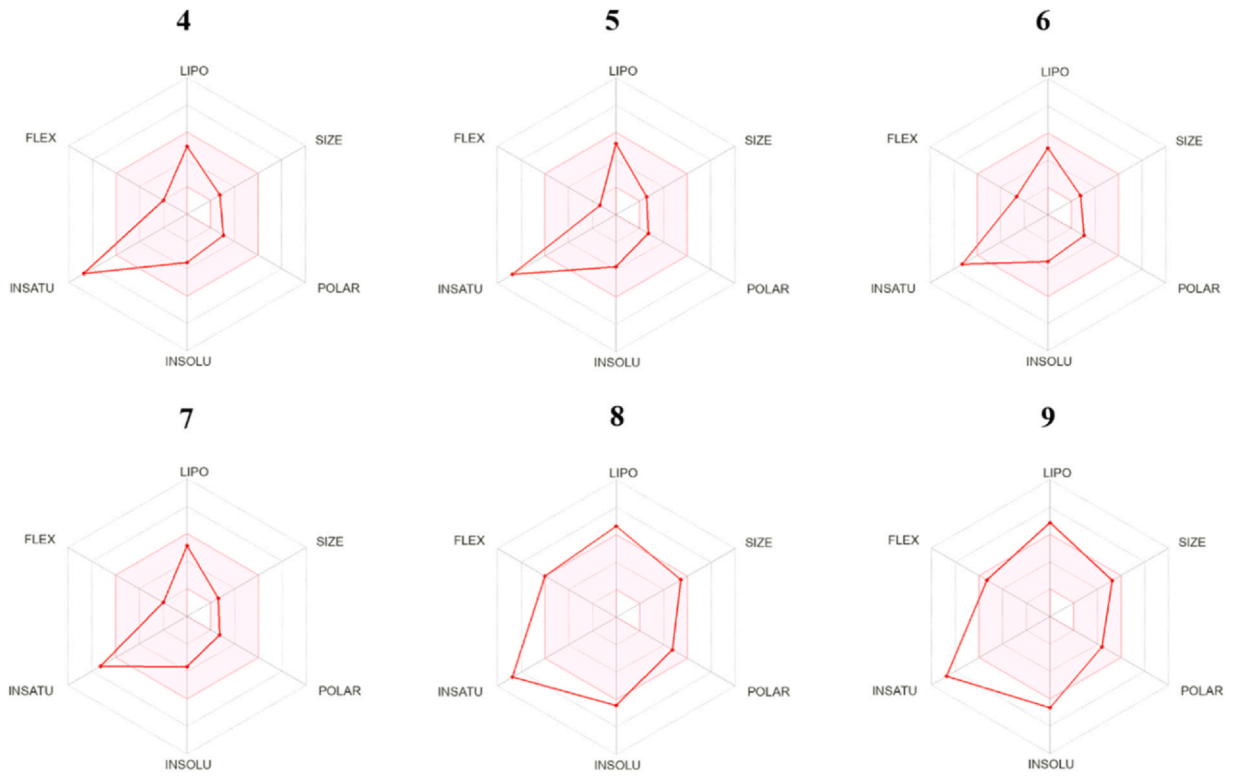

Fig. 5. Bioavailability radars of all synthesized compounds **(4 – 9).**

narrow the enzyme's access pathway, restricting the entry of other molecules into the active site. Detailed interaction analysis reveals that these regions contribute to binding through multiple stabilizing interactions, which may support activity but do not solely determine experimental potency.

The molecular docking analysis of ligands **6** and **8** with the tyrosinase enzyme revealed that both compounds interact with key amino acid residues within the active site through hydrogen bonding, electrostatic interactions, and hydrophobic interactions. These interactions are essential for elucidating the binding mechanism and provide valuable insights into the molecular recognition between the ligands and the enzyme. Copper ions located in the catalytic region play a crucial role in the activity of the tyrosinase enzyme. These ions are stabilized by histidine residues. As illustrated in Fig. 4, compounds **6** and **8** engage with the enzyme's active site as well as the region near the copper ion. The amino acids His61, His85, His94, His259, His263, and His296 within the active site of the tyrosinase enzyme play a key role in the binding of tropolone to this region[69]. Analysis of the docking results for compounds **6** and **8** revealed notable similarities with the reference molecule tropolone, as they docked through interactions with the active site residues His61, His85, and His263. These findings indicate a qualitative consistency between the in vitro results and the in silico binding modes.

3.6. ADME prediction results

ADME examines the processes of drug absorption, distribution, metabolism, and excretion in an organism using mathematical models. Since pharmacodynamic research plays a crucial role in the drug development process, it has a significant impact on drug design[70].

Fig. 5 displays the bioavailability radar plots for the synthesized compounds (**4–9**). The shaded pink area delineates the desirable range for six key parameters: lipophilicity (Lipo), molecular weight (Size), topological polar surface area (Polar), water insolubility (Insolu), degree of unsaturation (Insatu), and molecular flexibility (Flex). Furthermore, this investigation encompassed a comprehensive evaluation of the compounds' physicochemical attributes, including their lipophilicity, aqueous solubility, pharmacokinetic behavior, drug-likeness potential, and toxicity profiles. Radar deviations are primarily due to the saturation descriptor, which can negatively affect solubility and thus oral exposure; however, since oral bioavailability is multifactorial, this trend can be considered indicative.

All the compounds exhibited notable structural flexibility, featuring between 2 and 9 rotatable bonds (RBs). Each compound had fewer than 10 hydrogen bond acceptors (HBAs) and less than 5 hydrogen bond donors (HBDs), reflecting a favorable HBD-to-HBA balance, which is beneficial for oral bioavailability. The topological polar surface area (TPSA) values of the compounds were all within the optimal range of 0–140, supporting both efficient gastrointestinal absorption and oral bioavailability. Except for

Table 5
Predicted drug similarity parameters of thiophene-based Schiff bases obtained from ADME analysis.

Property	4	5	6	7	8	9
Molecular Weight (g/mol)	217.29	201.29	219.30	203.30	451.48	435.48
H-bond acceptors	2	1	1	0	4	3
H-bond donors	0	0	1	1	1	1
Rotatable Bonds	3	2	4	3	9	8
Lipophilicity (LOGP)	3.959	4.411	3.001	3.496	4.267	4.546
Fraction Csp^3	0.08	0.08	0.17	0.17	0.08	0.08
TPSA ($Å^2$)	21.590	12.360	21.260	12.030	56.790	47.560
Water Solubility (Log S/ESOL)	-3.55	-3.81	-3.43	-3.68	-6.43	-6.67
Gastrointestinal Absorption	High	High	High	High	Low	Low
BBB Permeability	Yes	Yes	Yes	Yes	No	No
Skin permeation (Log K_p) (cm/s)	-5.35	-4.97	-5.44	-5.07	-4.73	-4.35
P-gp Substrate	No	No	No	No	Yes	Yes
Plasma protein binding (PPB) (%)	97.369	97.407	96.621	96.734	99.762	99.934
Synthetic accessibility	2.36	2.45	1.79	1.76	4.52	4.48
Lipinski	Yes; 0 violation	Yes; 0 violation	Yes; 0 violation	Yes; 0 violation	Yes; 0 violation	Yes; 0 violation
Ghose	Yes	Yes	Yes	Yes	No;1violation: WLOGP > 5.6	No;1 violation: WLOGP > 5.6
Veber	Yes	Yes	Yes	Yes	Yes	Yes
Muegge	Yes	Yes	Yes	Yes	No;1 violation: XLOGP3 > 5	No; 1 violation: XLOGP3 > 5

compounds **8** and **9**, all other molecules displayed satisfactory gastrointestinal absorption. Regarding solubility, all compounds —except compounds **8** and **9**— showed good water solubility, with Log S values ranging from –3.43 to –6.67. Synthetic accessibility (SA) scores ranged from 1 (very easy) to 10 (extremely difficult), indicating that most compounds are relatively easy to synthesize, handle, and formulate.

In silico ADME predictions suggested that compounds **4**, **5**, **6** and **7** may possess blood–brain barrier (BBB) permeability. This property should be interpreted cautiously, as BBB penetration is not necessarily required for the intended therapeutic applications. Recent studies have reported that BBB-permeable small molecules may interact with central nervous system (CNS) targets; therefore, further experimental evaluation is recommended to better understand the CNS exposure and safety profile of these compounds[71–74]. In this context, the predicted BBB permeability of compounds **4**, **5**, **6** and **7** highlights a pharmacokinetic aspect that may be explored and clarified in future studies rather than representing a definitive therapeutic advantage or limitation. Additionally, all compounds except **8** and **9** were predicted to be P-glycoprotein (P-gp) substrates. Compounds **8** and **9** also exhibited more than 99% plasma protein binding (PPB), which is typically associated with a low therapeutic index due to reduced levels of unbound drug in plasma, although these values still comply with drug-likeness criteria. The skin permeability (Log Kp) values of the compounds ranged between –4.35 and –5.44 cm/s, where a lower value indicates reduced skin permeability. For instance, compound **6** showed the lowest skin permeability (Log Kp = –5.44 cm/s), while compound **9** exhibited higher permeability (Log Kp = –2.12 cm/s) (Table 5). Overall, according to Lipinski, Ghose, Veber, and Muegge guidelines, all compounds possessed the necessary physicochemical properties required for drug development.

4. Conclusion

This study reports the synthesis of a series of thiophene-based Schiff bases by microwave method, their reduction and the successful synthesis of α-aminophosphonate derivatives. The structures of all synthesized compounds were characterized using NMR spectroscopy and elemental analysis techniques. In addition to the synthetic studies, the inhibitory effects of these compounds on α-glucosidase and tyrosinase enzymes were investigated. Compounds **6** and **8**, which are thiophene-based Schiff bases, exhibited a moderate level of tyrosinase inhibition when compared to the standard inhibitor kojic acid, with IC_{50} values of 110.02 and 69.32 μM, respectively. Our findings reveal a new class of enzyme inhibitors that exhibit biological activity on α-glucosidase and tyrosinase enzymes. Density Functional Theory (DFT) studies were conducted to better understand the electronic and molecular properties of the compounds. Based on the results obtained from *in vitro* studies, molecular docking studies were conducted to gain a more detailed understanding of the interactions between the two most active compounds and the active sites of the target enzymes. The results obtained from *in vitro* and *in silico* studies revealed that the synthesized compounds have strong interactions with the active sites of the target enzymes. Furthermore, ADME studies were performed for all compounds. The obtained results demonstrate that these compounds have the potential for pharmaceutical development. The combination of both experimental and computational results shows that these new thiophene-based heterocyclic compounds (**4–9**) have promising potential as effective enzyme inhibitors. These findings provide a significant contribution to the field of multi-target drug discovery, providing new candidate compounds for the treatment of diabetes and skin diseases. Structural optimization studies will continue to increase selectivity and minimize off-target effects. Thus, it is aimed to take an important step towards the development of more effective therapeutic agents.

Funding

The authors received no financial support for the research, authorship, and publication of this article.

Ethics approval and consent to participate

Not applicable.

CRediT authorship contribution statement

Emel Ekinci: Writing – original draft, Visualization, Validation, Methodology, Investigation, Conceptualization. **Özlem Gündoğdu Aytaç:** Writing – review & editing, Visualization, Supervision, Methodology, Investigation, Conceptualization. **Kübra Öztürk:** Writing – original draft, Investigation, Conceptualization. **Sertan Aytaç:** Writing – review & editing, Methodology, Investigation, Conceptualization. **Harun Çiftçi:** Supervision, Investigation, Conceptualization.

Data availability statement

The datasets used and analysed during the current study are available from the corresponding author on reasonable request.

Declaration of Competing Interest

The authors declare that they have no known competing financial interests or personal relationships that could have appeared to influence the work reported in this paper.

Acknowledgments

The authors would like to thank Kırşehir Ahi Evran University for the facilities and technical support. The computations reported in this study were partially performed at TUBITAK ULAKBIM High Performance and Grid Computing Center (TRUBA resources).

References

1. Chakraborty R, Roy S, Mandal V. Assessment of traditional knowledge of the antidiabetic plants of Darjeeling and Sikkim Himalayas in the context of recent phytochemical and pharmacological advances. *J Integr Med.* 2016;14:336–358.
2. Mi W, Xia Y, Bian Y. The influence of ICAM1 rs5498 on diabetes mellitus risk: evidence from a meta-analysis. *Inflamm Res.* 2019;68:275–284.
3. Su M, Tang T, Tang W, Long Y, Wang L, Liu M. Astragalus improves intestinal barrier function and immunity by acting on intestinal microbiota to treat T2DM: a research review. *Front Immunol.* 2023;14:1243834.
4. Wu H, Deng X, Shi Y, Su Y, Wei J, Duan H. PGC-1α, glucose metabolism and type 2 diabetes mellitus. *J Endocrinol.* 2016;229:R99–R115.
5. Kolseth IBM, Reine TM, Parker K, et al. Increased levels of inflammatory mediators and proinflammatory monocytes in patients with type I diabetes mellitus and nephropathy. *J Diabetes Complicat.* 2017;31:245–252.
6. Gupta A, Behl T, Sehgal A, et al. Exploring the recent molecular targets for diabetes and associated complications. *Mol Biol Rep.* 2021;48:2863–2879.
7. Deng Y, Huang L, Zhang C, et al. Skin-care functions of peptides prepared from Chinese quince seed protein: sequences analysis, tyrosinase inhibition and molecular docking study. *Ind Crops Prod.* 2020;148:112331.
8. Sun H, Saeedi P, Karuranga S, et al. IDF Diabetes Atlas: Global, regional and country-level diabetes prevalence estimates for 2021 and projections for 2045. *Diabetes Res Clin Pract.* 2022;183:109119.
9. Sevimli E, Seyhan G, Akkaya D, Sarı S, Barut B, Köksoy B. Effective α-glycosidase inhibitors based on polyphenolic benzothiazole heterocycles. *Bioorg Chem.* 2024;147:107366.
10. Min X, Guo S, Lu Y, Xu X. Investigation on the inhibition mechanism and binding behavior of cryptolepine to α-glucosidase and its hypoglycemic activity by multi-spectroscopic method. *J Lumin.* 2024;269:120437.
11. Proença C, Ribeiro D, Freitas M, Fernandes E. Flavonoids as potential agents in the management of type 2 diabetes through the modulation of α-amylase and α-glucosidase activity: a review. *Crit Rev Food Sci Nutr.* 2022;62:3137–3207.
12. Ledwoń P, Goldeman W, Hałdys K, et al. Tripeptides conjugated with thiosemicarbazones: new inhibitors of tyrosinase for cosmeceutical use. *J Enzym Inhib Med Chem.* 2023;38:2193676.
13. Panzella L, Napolitano A. Natural and bioinspired phenolic compounds as tyrosinase inhibitors for the treatment of skin hyperpigmentation: Recent advances. *Cosmetics.* 2019;6:57.
14. Böhm M. *Disorders of melanin pigmentation. Braun-Falco´s Dermatology*. Springer; 2021:1–35.
15. Zolghadri S, Bahrami A, Hassan Khan MT, et al. A comprehensive review on tyrosinase inhibitors. *J Enzym Inhib Med Chem.* 2019;34:279–309.
16. Dettori MA, Fabbri D, Dessì A, et al. Synthesis and studies of the inhibitory effect of hydroxylated phenylpropanoids and biphenols derivatives on tyrosinase and laccase enzymes. *Molecules.* 2020;25:2709.
17. Visvanathan R, Houghton MJ, Barber E, Williamson G. Structure-function relationships in (poly) phenol-enzyme binding: direct inhibition of human salivary and pancreatic α-amylases. *Food Res Int.* 2024;188:114504.
18. İmamoğlu R, Koc E, Kısa D. Polyphenolic compounds: Synthesis, assessment of antimicrobial effect and enzymes inhibition against important medicinal enzymes with computational details. *Bioorg & Med Chem Lett.* 2022;65:128722.
19. Machida S, Mukai S, Kono R, Funato M, Saito H, Uchiyama T. Synthesis and comparative structure–activity study of carbohydrate-based phenolic compounds as α-glucosidase inhibitors and antioxidants. *Molecules.* 2019;24:4340.
20. Jampilek J. *Heterocycles in Medicinal Chemistry*. Molecules; 2019;24:3839.
21. Heravi MM, Zadsirjan V. Prescribed drugs containing nitrogen heterocycles: an overview. *RSC Adv.* 2020;10:44247–44311.
22. Yan Z, Yu B, Lan X, et al. Synthesis, bioactivity evaluation and theoretical study of nicotinamide derivatives containing diphenyl ether fragments as potential succinate dehydrogenase inhibitors. *J Mol Struct.* 2024;1308:138331.
23. Sarı N, Altundas A, Ogutcu H. Determination of protonation and complexation constants of cyclic alkyl thiophene-schiff bases with Ni(II) Ion, Süleyman Demirel. *Univ Fac Arts Sci J Sci.* 2011;6:55–61.
24. Mehdhar FS, Alzahrani AY, Abdel-Galil E, Abdel-Ghani GE, Saeed A, Abdel-Latif E. Synthesis of some new thiophene-based compounds and evaluations of their cytotoxic activities. *Bull Chem Soc Ethiop.* 2023;37:373–389.
25. Zhao M, Cui Y, Zhao L, et al. Thiophene derivatives as new anticancer agents and their therapeutic delivery using folate receptor-targeting nanocarriers. *ACS Omega.* 2019;4:8874–8880.
26. Aytaç S. Eco-friendly synthesis of new thiophene-based schiff bases containing piperidine rings. *Org Commun.* 2024;2:128–132.
27. Ekinci E, Çiftçi H, Adem Ş, Aytaç Ö.G, Eyüpoğlu V. A comprehensive investigation of Schiff bases and bis-α-aminophosphonates as potent agents against Alzheimer's disease by computer-aided drug discovery techniques and in vitro examinations. *J Mol Struct.* 2025;1333:141734.
28. Ozturk K, Tanyildizi MS, Ciftci H, Aytac OG. Synthesis of thiophene-based imine and phosphoazometine compounds: in vitro antiproliferative, antimicrobial, antioxidant, carbonic anhydrase I and II enzyme inhibition evaluations and molecular docking study. *Chem Pap.* 2025:1–17.
29. Warad I, Ali O, Al Ali A, et al. Synthesis and spectral Identification of three Schiff bases with a 2-(piperazin-1-yl)-N-(thiophen-2-yl methylene) ethanamine moiety acting as novel pancreatic lipase inhibitors: thermal, DFT, antioxidant, antibacterial, and molecular docking investigations. *Molecules.* 2020;25:2253.
30. Aytac S, Gundogdu O, Bingol Z, Gulcin İ. Synthesis of Schiff bases containing phenol rings and investigation of their antioxidant capacity, anticholinesterase, butyrylcholinesterase, and carbonic anhydrase inhibition properties. *Pharmaceutics.* 2023;15:779.
31. Ünver Y, Deniz S, Çelik F, Akar Z, Küçük M, Sancak K. Synthesis of new 1, 2, 4-triazole compounds containing Schiff and Mannich bases (morpholine) with antioxidant and antimicrobial activities. *J Enzym Inhib Med Chem.* 2016;31:89–95.
32. Ünver Y, Sancak K, Çelik F, et al. New thiophene-1, 2, 4-triazole-5 (3)-ones: Highly bioactive thiosemicarbazides, structures of Schiff bases and triazole–thiols. *Eur J Med Chem.* 2014;84:639–650.
33. Nayab S, Alam A, Ahmad N, et al. Thiophene-derived Schiff base complexes: synthesis, characterization, antimicrobial properties, and molecular docking. *ACS Omega.* 2023;8:17620–17633.
34. Çelik F, Ünver Y. 1, 2, 4-Triazole derivative containing thiophen ring: comparison of theoretical IR and NMR data with experimental. *J Indian Chem Soc.* 2022;99:100455.
35. Süleymanoğlu N, Demir EE, Direkel Ş, Ünver Y. Theoretical study and antimicrobial activities of New Schiff base derivatives with thiophene. *J Mol Struct.* 2020;1218:128522.
36. Alaşalvar C, Soylu MS, Ünver Y, Apaydın G, Ünlüer D. Spectroscopy studies, X-ray diffraction and DFT, HF calculations of 4-allyl-5-(thiophen-2-ylmethyl)-2H-1, 2, 4-triazol-3 (4H)-one. *J Mol Struct.* 2013;1033:243–252.
37. Naydenova ED, Todorov PT, Mateeva PI, Zamfirova RN, Pavlov ND, Todorov SB. Synthesis and biological activity of novel small peptides with aminophosphonates moiety as NOP receptor ligands. *Amino Acids.* 2010;39:1537–1543.
38. Bhattacharya AK, Rana KC, Pannecouque C, De Clercq E. An efficient synthesis of a hydroxyethylamine (HEA) isostere and its α-aminophosphonate and phosphoramidate derivatives as potential anti-HIV agents. *ChemMedChem.* 2012;7:1601–1611.
39. Fernandez-Perez H, Etayo P, Panossian A, Vidal-Ferran A. Phosphine− phosphinite and phosphine− phosphite ligands: preparation and applications in asymmetric catalysis. *Chem Rev.* 2011;111:2119–2176.
40. Kim S, Park B, Lee GS, Hong SH. Synthesis of α-aminoacetals via decarboxylative coupling of imine and 2, 2,-diethoxyacetic acid. *J Org Chem.* 2022;88:6532–6537.

41. Tabane TH, Singh GS. A simple reduction of imines to biologically important secondary amines using sodium borohydride/alumina in solid-phase. *Proc Natl Acad Sci India Secti A: Phys Sci.* 2014;84:517–521.
42. López FI, de la Cruz FN, López J, et al. A simple method for the synthesis of 1, 3-diaminopropan-2-ols derivatives and their ex vivo relaxant activity on isolated rat tracheal rings. *Med Chem Res.* 2017;26:1325–1335.
43. Patel G, Patel AR, Lambat TL, Banerjee S. Direct one-pot synthesis of imines/benzothiazoles/benzoxazoles from nitroarenes via sequential hydrogenation-condensation using Nano-NiFe2O4 as catalyst under microwave irradiation. *Curr Res Green Sustain Chem.* 2021;4:100149.
44. Patil S, Bedre A, Gade V, Jopale M, Bhagat R, Pise A. One-pot protocol for the reductive amination of aldehydes using thiamine hydrochloride as a green catalyst under solvent-free condition. *Synth Commun.* 2023;53:1545–1558.
45. Aytaç S, Aytaç Ö.G. Eco-friendly synthesis of new thiophene-based Schiff bases containing piperidine rings, Organic. *Communications.* 2024;17:132.
46. Aytaç S. Synthesis of pyridine-based imine compounds and molecular docking studies against dopamine D2 receptors. *Hittite J Sci Eng.* 2023;10:161–165.
47. Ayaz M, Gündoğdu Ö, Aytaç S, Erdem B, Çiftçi H, Erdogdu Y. Microwave-assisted synthesis, characterizations, antimicrobial activities, and DFT studies on some pyridine derived Schiff bases. *J Mol Struct.* 2022;1269:133791.
48. Aytaç S. Resynthesis of Schiff base compounds with an environmentally friendly method. *J Inst Sci Technol.* 2021;11:2979–2991.
49. Fondo M, Corredoira-Vázquez J, García-Deibe AM, Sanmartín-Matalobos J. *An easy approach to obtain alcohol-amines by reduction of alcohol functionalized imines. Proceedings*. Proceedings; 2019;9:2.
50. Varga PR, Keglevich G. Synthesis of α-aminophosphonates and related derivatives; the last decade of the Kabachnik–Fields reaction. *Molecules.* 2021;26:2511.
51. Kurşun-Aktar BS, Adem G, Tatar-Yilmaz ZAH, Hameed EE, Oruç-Emre. Investigation of α-glucosidase and α-amylase inhibitory effects of phenoxy chalcones and molecular modeling studies. *J Mol Recognit.* 2023;36:e3061.
52. Aydinli E, Hameed ZA, Goksu H, Adem S. Investigation of the efficacy on tyrosinase enzyme of 5-substituted-1H-tetrazole derivatives synthesized with Pd-containing nanoparticle. *J Chem Sci.* 2024;136:22.
53. Becke AD. Density-functional thermochemistry. III. The role of exact exchange. *J Chem Phys.* 1993;98:5648–5652.
54. Lee C, Yang W, Parr RG. Development of the Colle-Salvetti correlation-energy formula into a functional of the electron density. *Phys Rev B.* 1988;37:785.
55. Dunning TH. Jr, Gaussian basis sets for use in correlated molecular calculations. I. The atoms boron through neon and hydrogen. *J Chem Phys.* 1989;90:1007–1023.
56. Thomsen R, Christensen MH. MolDock: a new technique for high-accuracy molecular docking. *J Med Chem.* 2006;49:3315–3321.
57. Xiong G, Wu Z, Yi J, et al. ADMETlab 2.0: an integrated online platform for accurate and comprehensive predictions of ADMET properties. *Nucleic Acids Res.* 2021;49:W5–W14.
58. Daina A, Michielin O, Zoete V. SwissADME: a free web tool to evaluate pharmacokinetics, drug-likeness and medicinal chemistry friendliness of small molecules. *Sci Rep.* 2017;7:42717.
59. Manda BR, Potuganti GR, Alla M. Synthesis of Tröger's base bis (α-aminophosphonate) derivatives. *ARKIVOC.* 2016:246–260.
60. Schweiker SS, Tauber AL, Kam CM, Eyckens DJ, Henderson LC, Levonis SM. α-aminophosphonates as potential PARP1 inhibitors. *ChemistrySelect.* 2020;5:4205–4209.
61. Varga PR, Keglevich G. The last decade of optically active α-aminophosphonates. *Molecules.* 2023;28:6150.
62. Uma Maheswara Rao K, Namkoong S, Yu HC, Park J, Chung CM, Oh SY. Green synthesis and biological evaluation of new di-α-aminophosphonate derivatives as cytotoxic agents. *Arch der Pharm.* 2013;346:851–859.
63. Kim H-D, Choi H, Abekura F, et al. Naturally-occurring tyrosinase inhibitors classified by enzyme kinetics and copper chelation. *Int J Mol Sci.* 2023;24:8226.
64. Ali TE, Assiri MA, Hussien M, El-Tantawy El Sayed I. Recent advances in the synthesis of dialkyl (aryl) α-(aryl/heterocyclic/heteroaryl-α-(aryl/heteroarylamino) phosphonates. *Curr Org Chem.* 2023;27:1484–1503.
65. Kandula MKR, Gundluru M, Nemallapudi BR, et al. Synthesis, antioxidant activity, and α-glucosidase enzyme inhibition of α-aminophosphonate derivatives bearing piperazine-1, 2, 3-triazole moiety. *J Heterocycl Chem.* 2021;58:172–181.
66. Pavan Phani Kumar M, Vejendla A, Gladis Raja Malar C, Chennamsetty S, Talari S, Vedula N. silico molecular docking study and nano TiO2-SiO2 catalyzed microwave facilitated synthesis of new bis (α-aminophosphonates) as potential anti-diabetic agents. *Phosphorus Sulfur Silicon Relat Elem.* 2023;198:808–821.
67. Yurdakul S. Tanrıbuyurdu, Theoretical and experimental study of solvent effects on the structure, vibrational spectra, and tautomerism of 3-amino-1, 2, 4-triazine. *J Mol Struct.* 2013;1052:57–66.
68. Kumar CC, Balachandran V, Fun H-K, Chandraju S, Quah CK. Synthesis, crystal growth, single crystal X-ray analysis and vibrational spectral studies of (2*E*)-3-(2-chloro-4-fluorophenyl)-1-(3, 4-dimethoxyphenyl) prop-2-en-1-one: a combined DFT study. *J Mol Struct.* 2015;1100:299–310.
69. Yamamoto K, Miyake H, Kusunoki M, Osaki S. Crystal structures of isomaltase from Saccharomyces cerevisiae and in complex with its competitive inhibitor maltose. *FEBS J.* 2010;277:4205–4214.
70. Alyar S, Özmen Ü.Ö, Erdem K, Alyar H. Synthesis, molecular docking study, molecular dynamics simulation and ADMET prediction of new Sulfa drugs having CA II inhibitory effect and antidiabetic activity. *J Mol Struct.* 2025;1336:142015.
71. Arshad S, Maalik A, Rehman W, et al. Facile indazole-endowed thiadiazole hybrid derivatives as antibacterial, anti-diabetic and thymidine phosphorylase inhibitors: an insight to experimental, in-vitro biological potential and computational approaches. *Saudi Pharm J.* 2025;33:20.
72. Khan Y, Maalik A, Rehman W, et al. Facile 3-chloro-1H-indazole based 1,3,4-thiadiazole derivatives as novel thymidine phosphorylase and anti-diabetic inhibitors: experimental, in-vitro and molecular modelling approaches. *Naunyn-Schmiedeberg's Arch Pharmacol.* 2026;399:833–851.
73. Khan Y, Mukhtiar A, Sarfraz H, et al. Unveiling of the novel benzothiazole derived thiazolidinone derivatives: in vitro and in silico insights to design a promising agent for anti-Alzheimer's disease. *Z FüR Naturforsch C.* 2025;81:75–93.
74. Khan Y, Hussain R, Rehman W, et al. In-vitro and in-silico assessment of thiazole-thiazolidinone derivatives as selective inhibitors of urease and α-glucosidase. *Future Med Chem.* 2024;16:2627–2636.